Science in China Series D: Earth Sciences

www.scichina.com
earth.scichina.com
www.springerlink.com

Petrogenesis of highly fractionated I-type granites in the Zayu area of eastern Gangdese, Tibet: Constraints from zircon U-Pb geochronology, geochemistry and Sr-Nd-Hf isotopes

ZHU DiCheng[1†], MO XuanXue[1], WANG LiQuan[2], ZHAO ZhiDan[1], NIU Yaoling[3], ZHOU ChangYong[2] & YANG YueHeng[4]

[1] State Key Laboratory of Geological Processes and Mineral Resources, and School of Earth Science and Resources, China University of Geosciences, Beijing 100083, China;
[2] Chengdu Institute of Geology and Mineral Resources, Chengdu 610082, China;
[3] Department of Earth Sciences, Durham University, Durham DH1 3LE, UK;
[4] Institute of Geology and Geophysics, Chinese Academy of Sciences, Beijing 100029, China

The Cretaceous granitoids in the middle and northern Gangdese, Tibet are generally interpreted as the products of anatexis of thickened deep crust genetically associated with the Lhasa-Qiangtang collision. This paper reports bulk-rock major element, trace element and Sr-Nd isotopic data, zircon U-Pb age data, and zircon Hf isotopic data on the Zayu pluton in eastern Gangdese, Tibet. These data shed new light on the petrogenesis of the pluton. Our SHRIMP zircon U-Pb age dates, along with LA-ICPMS zircon U-Pb age dates recently reported in the literature, indicate that the Zayu pluton was emplaced at about 130 Ma, coeval with Early Cretaceous magmatic rocks in other areas of eastern Gangdese (e.g., Rawu, Baxoi areas) and the Middle Gangdese. The Zayu pluton samples lack amphibole and muscovite, and are compositionally characterized by high SiO_2 (69.9%—76.8%), K_2O (4.4%—5.7%), and low P_2O_5 (0.05%—0.12%). These samples also have A/CNK values of 1.00—1.05, and are enriched in Rb, Th, U, and Pb, and depleted in Ba, Nb, Ta, Sr, P, Ti, and Eu. These geochemical features suggest that the Zayu pluton samples are metaluminous to slightly peraluminous and are of highly fractionated I-type granite. The Zayu pluton samples have high $\varepsilon_{Nd}(t)$ values (–10.9—–7.6) and low initial $^{87}Sr/^{86}Sr$ ratios (0.7120—0.7179) relative to melts derived from mature continental crust in the Gangdese (e.g., Ningzhong Early Jurassic strongly peraluminous granite). The Zayu pluton samples are heterogeneous in zircon $\varepsilon_{Hf}(t)$ values (–12.8—–2.9), yielding ancient zircon Hf crustal model ages of 1.4—2.0 Ga. The data obtained in this study together with the data in the recent literature suggest that the Early Cretaceous granitoids in eastern Gangdese represent the eastward extension of the Early Cretaceous magmatism in the middle Gangdese, and that the Lhasa micro-continent block with ancient basement may extend for ~2000 km from east to west. Zircon Hf isotopic data and bulk-rock zircon saturation temperature (789—821℃) indicate that mantle-derived materials likely played a role in the generation of the Zayu pluton. We propose that the Zayu pluton was most likely generated in a setting associated with southward subduction of the Bangong-Nujiang ocean floor, where mantle wedge-derived magmas may have provided

Received April 8, 2009; accepted August 5, 2009
doi: 10.1007/s11430-009-0132-x
†Corresponding author (email: dchengzhu@163.com)
Supported by National Natural Science Foundation of China (Grant Nos. 40572051, 40830317, 40873023, 40672044), National Basic Research Program of China (Grant No. 2009CB421002), Chinese "111" Project (Grant No. B07011), and Programme of the Integrated Study of Basic Geology of Qinghai-Tibetan Plateau of the China Geological Survey

Citation: Zhu D C, Mo X X, Wang L Q, et al. Petrogenesis of highly fractionated I-type granites in the Zayu area of eastern Gangdese, Tibet: Constraints from zircon U-Pb geochronology, geochemistry and Sr-Nd-Hf isotopes. Sci China Ser D-Earth Sci, 2009, 52(9): 1223-1239, doi: 10.1007/s11430-009-0132-x

the heat and material for the anatexis of ancient crust of the Lhasa micro-continent, resulted in hybrid melts (i.e., mantle-derived basaltic magmas + crust-derived felsic magmas). Such hybrid melts with subsequent fractional crystallization are responsible for the highly evolved Zayu pluton (crust thickening is not a prerequisite).

zircon U-Pb dating, Sr-Nd-Hf isotope, highly fractionated I-type granite, Zayu pluton, eastern Gangdese, Tibet

It was generally thought that granites with high $\varepsilon_{\mathrm{Nd}}(t)$ values and young Nd model ages are derived from either recycled juvenile crust or nascent mantle input into the continental crust[1,2], whereas granites with low $\varepsilon_{\mathrm{Nd}}(t)$ values and old Nd model ages are generated by the anatexis or remelting of pre-existed ancient crustal materials[3]. While this traditional concept has been widely accepted, its validity needs testing. This is because most granites, including strongly peraluminous granite and rhyolite (including S-type granite), are hybrid melts with variable contributions of mantle-derived materials[4−9], rather than pure crust-derived melts as previously thought. It has been noted that granite magmas are primarily water-unsaturated[10], and their generation is mainly controlled by heating and decompression. Therefore, extensive granitoid magmatism is generally associated with subduction zones or syn- and post-collisional processes along orogenic belt[8]. This concept is important in studying magma genesis and mantle-crust interaction in general and in understanding geodynamic settings of the extensive Cretaceous granitoid magmatism in the Middle and northern Gangdese in particular. Different models have been proposed for the petrogen- esis of these rocks so far, including: (1) partial melting of upper crust and deep-level crust or upper mantle above a post-collision subduction zone[11], (2) anatexis of thickened crust during the Lhasa-Qiangtang collision[12], and (3) anatexis of thickened crust after the Lhasa-Qiangtang collision[13]. A likely reason for these diverse models is the lack of high-quality geochronological and geochemical data pertaining to the Cretaceous magmatic rocks in the middle and northern Gangdese. As part of a systematic study of the Cretaceous magmatism in the middle and northern Gangdese, this paper reports bulk-rock major element, trace element and Sr-Nd isotope data, zircon U-Pb age data, and zircon Hf isotopic data on the Zayu pluton in the eastern Gangdese. These new data, together with the recent literature data1),2), offer important constraints on the petrogenesis and geodynamic setting of the Zayu pluton.

1 Geological setting and samples

The Tibetan Plateau is generally divided, from north to south, into the Songpan-Garzê flysch complex, and several tectonic blocks (i.e., Qiangtang, Gangdese, and the Himalaya blocks), separated by the Jinsha (JSSZ), Bangong-Nujiang (BNSZ), and Yarlung Zangbo (YZSZ) suture zones, respectively (Figure 1(a)). On the basis of well-preserved geological records, the western and central parts of the Gangdese with a width of 200−300 km can be further divided (from north to south) into the northern Gangdese (NG), middle Gangdese (MG), Gangdese Retro-arc Uplift Belt (GRUB), and southern Gangdese (SG), separated by the Shiquan River-Nam Co Mélange Zone (SNMZ), Gar-Longgar-Cuomai Fault (GLCF), and Luobadui-Mila Mountain Fault (LMF), respectively (Figure 1(b))[16,17]. The northern Gangdese consists mainly of Jurassic-Cretaceous volcano-sedimentary strata and associated intrusive rocks, along with probable presence of Cambrian or Neoproterozoic crystalline basement in the Amdo area[12,18]. The crust of the northern Gangdese was shortened by > 50% during the Late Cretaceous-Paleocene[19,20]. The middle Gangdese extends more than 1000 km E-W and is dominated by the Zenong Group (Lower Cretaceous) and minor Jienu Group (Mid-Upper Jurassic), Jiega Formation (Lower Cretaceous) volcano-sedimentary strata, along with minor Paleozoic strata in Xainza and Coqen areas (Figure 1(b)). Numerous felsic volcanic rocks, volcanoclastic rocks, and associated intrusive rocks are present in the middle Gangdese. The Gangdese Retro-arc Uplift Belt

1) Zhu D C, Mo X X, Niu Y, et al. The lithospheric architecture of the Lhasa Terrane: Revelation and geodynamic significance, 2009.

2) Zhu D C, Mo X X, Niu Y, et al. Zircon U-Pb dating and Hf isotopic investigation on the Early Cretaceous igneous rocks along a west-east traverse throughout the central Lhasa Terrane, Tibet. CHem Geol, 2009.

consists mainly of Carboniferous-Permian metasedimentary rocks and minor Triassic sedimentary rocks, along with abundant Mesozoic intrusive rocks in the eastern part of this belt and rare Neoproterozoic metamorphic rocks in the Nyainqêntanglha area[21]. This belt was thrust southward over the southern Gangdese along the Luobadui-Mila Mountain Fault. The southern Gangdese is dominated by Cretaceous-Paleogene Gang- dese batholith and Paleogene-Eocene Linzizong volc- anic rocks, with minor Jurassic-Cretaceous sedimentary strata. The southern Gangdese experienced a major crustal shortening (>40%) and deformation during the Late Cretaceous-earliest Tertiary[22]. The area to the north of the southern Gangdese is generally referred to as the northern magmatic belt in the literature[23−26]. The strong deformation and tectonism of eastern Gangdese caused by the northward wedged eastern Himalayan Syntaxis have resulted in a narrowed Gangdese (Figure 1(b)) and a poor preservation of geological records relative to the western and central parts of this belt. This tectonic complexity has led to the question how the Gangdese tectonic units extend to the east.

The Gangdese is generally thought to represent not only a Cenozoic orogenic belt related to the India-Asia collision, but also a Mesozoic Andean-style active continental margin associated with the northward subduction of the Neo-Tethyan oceanic floor[12,14,23,26 − 31]. However, polarity variation of Hf isotopes of zircons from the Mesozoic magmatic rocks sampled along a north-south traverse from Xigaze, via Namling, Lhozhag, and Xainza, to Nyima/Siling Co across the central Gangdese (Figure 1(b)) indicates that much of the Mesozoic magmatism in the Gangdese may have been associated with the southward subduction of the Bangong-Nujiang Ocean seafloor1).

In the eastern Gangdese, extensive Cretaceous granitoids and minor Ordovician, Jurassic, and Cenozoic granitoids are exposed in a NW-SE belt to the southwest of the Bangong-Nujiang Suture Zone[15,27,32,33], and croup out the Carboniferous-Permian, Devonian metasedimentary rocks, and Proterozoic metamorphic rocks[15,34]. The Cretaceous granitoids occur mostly as batholiths (locally as stocks) and consist mainly of monzogranite, with minor granodiorite, syenogranite, dioritic veins, and dioritic enclaves[15,32,33,35]. Monzogranite samples investigated in this study were collected from the Zayu pluton, ~30 km to the west of Zayu County (Figure 1(c)). The Zayu pluton occurs as a batholith and consists mainly of Cretaceous granitoids, with Ordovician granites[15] and minor early Paleocene granites[32]. The rock types of the Zayu Cretaceous granitoids are fine- to median-grained biotite monzogranite, biotite gneissose granite, and median-grained two-mica granite[27,36]. The Zayu Cretaceous monzogranites are massive, and fine- to median-grained, and mainly contain perthite (~35%), oligoclase (~25%, An = ~20), quartz (~30%), biotite (~5%—10%), and accessory minerals (e.g., sphene, apatite, and zircon). Amphibole and muscovite are absent in the monzogranites. Feldspars experienced weak sericitization and quartz

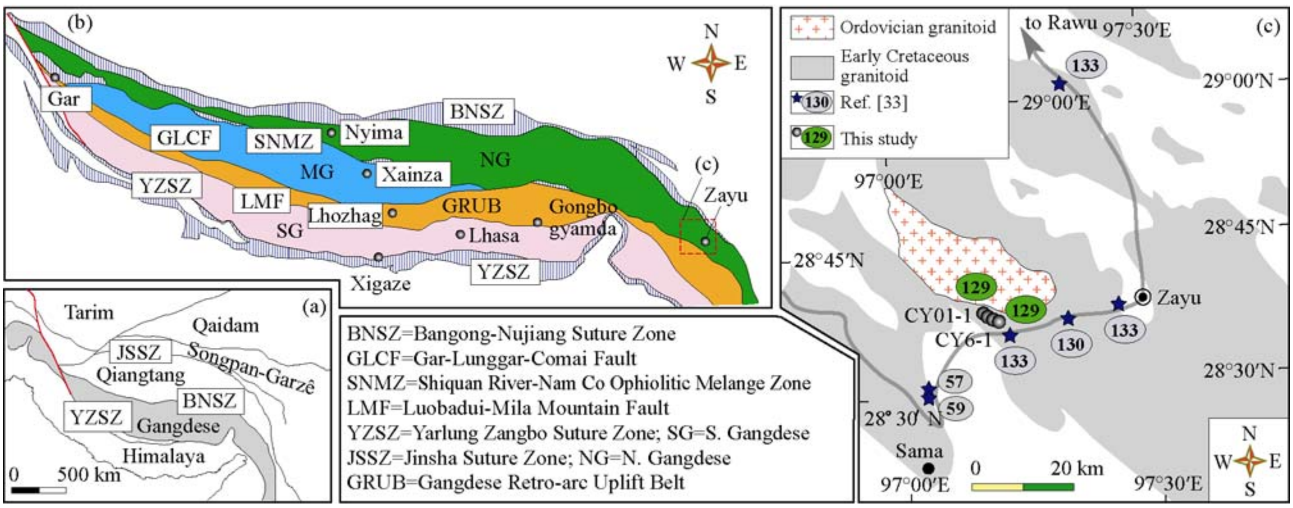

Figure 1 Tectonic outline of the Gangdese and Tibetan Plateau[14] and geological map of granitoids in Zayu area[15].

1) see 1) on page 1224.

exhibited clear cracked fabric. It should be noted that gabbroic veins with 0.5—2.0 m thick are present along joints within the monzogranites in the Zayu pluton. The gabbroic veins show a distinct contact with the monzogranites. Five zircons from a gabbro sample yield a Cameca 1280 U-Pb age of 62 Ma (our unpublished data), coeval with the early Paleocene granite (59—57 Ma)[32] in the northern Shama village (Figure 1(c)).

2 Analytical methods

Zircons were extracted by heavy-liquid and magnetic methods in the Laboratory of the Geological Team of Hebei Province, China. Cathodoluminescence (CL) images were taken under operation conditions of 15 kV and 4 nA, at the Institute of Geology, Chinese Academy of Geological Sciences, Beijing for inspecting zircon internal structures and for selecting positions for U-Pb dating. The SHRIMP zircon U-Pb dating was conducted at the Beijing SHRIMP center. The analytical spot size of ~30 μm was chosen during each analysis. The analytical conditions/procedures are given in ref. [37]. Measured compositions were corrected for common Pb using the ^{204}Pb-correction method. Uncertainties on individual analyses are reported as 1σ; mean ages for pooled ^{206}Pb/^{238}U results are reported as 2σ. The zircon U-Pb isotopic data are given in Table 1.

Bulk-rock major and trace element analyses were done at the State Key Laboratory of Continental Dynamics (SKLCD), Northwest University, Xi'an. During analysis, data quality was monitored by repeated analyses of USGS rock reference materials (BHVO-1, AGV-1, and G-2), together with regular monitoring of total procedural blanks. Major element analyses were done by XRF with analytical uncertainties generally better than 5%. Trace elements were determined using an Agilent 7500 a ICP-MS with analytical uncertainties generally better than 5%—10%. The analytical details are given in ref. [38]. Sample preparation for Sr and Nd analysis was also done at the SKLCD, while actual Sr-Nd isotopic analysis was done using a Finnigan MAT-261 mass spectrometer at China University of Geosciences (Wuhan). The detailed analytical procedures are given in ref. [39]. The measured ^{87}Sr/^{86}Sr and ^{143}Nd/^{144}Nd values were normalized to ^{86}Sr/^{88}Sr = 0.1194 and ^{146}Nd/^{144}Nd = 0.7219, respectively. During the analysis, the blanks are < 1 ng and < 50 pg for Sr and Nd, respectively; the average ^{143}Nd/^{144}Nd value of the La Jolla standard was 0.511862 ± 5 (2σ), and the average ^{87}Sr/^{86}Sr value of the NBS987 standard was 0.710236±16 (2σ). The bulk-rock geochemical data are given in Table 2.

Zircon Hf isotope analyses were subsequently done on the same spots using LA-MC-ICPMS with a beam size of 60 μm and laser pulse frequency of 8 Hz at the Institute of Geology and Geophysics, Chinese Academy of Sciences, Beijing. Details of instrumental conditions and data acquisition were given in refs. [42, 43]. During the analysis, ^{176}Hf/^{177}Hf and ^{176}Lu/^{177}Hf ratios of the standard zircon (91500) were 0.282286 ± 12 ($2\sigma_n$, n = 21), which is within the error obtained previously in this laboratory[42]. The $\varepsilon_{\rm Hf}(t)$ values were calculated based on zircon U-Pb age data of each spot using the ^{176}Lu decay constant of 1.867×10^{-11} a[44]. The zircon Hf isotope crustal model ages ($T_{\rm DM}{}^{\rm C}$) were calculated using the ^{176}Lu/^{177}Hf ratio (= 0.015[45]) of the average continental crust. The zircon Hf isotopic data are given in Table 3.

3 Results

3.1 Zircon U-Pb age

Two monzogranite samples (CY1-01, CY6-1) were selected for zircon SHRIMP U-Pb dating. The zircon U-Pb isotopic data are given in Table 1 and shown in Figure 2. Zircons from the two samples are mostly colorless and long prismatic (100—400 μm-long), with length/width ratios of 2∶1—4∶1. Twenty-seven zircons with clear oscillatory zoning (Figure 2(a) and (b)) from the two samples were analyzed using SHRIMP U-Pb method. One zircon from sample CY1-01 yields a ^{206}Pb/^{238}U age of 1062±22 Ma. However, this age is insignificant because it has very low Th and U (21 and 26 ppm, respectively) that will result in an unreliable value of ^{207}Pb. The remaining 26 analyses have 164—1671 ppm Th and 197—2603 ppm U with Th/U ratios of 0.29—1.16, consistent with their being of magmatic origin. The 13 analyses of sample CY1-01 plot on or close to the concordant curve and yield a weighted mean ^{206}Pb/^{238}U age of 129.1 ± 1.6 Ma (MSWD = 1.9) (Figure 2(c)), suggesting an emplacement age of 129 Ma. Nine analyses of sample CY6-1 yield a weighted mean ^{206}Pb/^{238}U age (128.5 ± 3.1 Ma) identical to that of sample CY1-01, although the data quality is not as good (Figure 2(d)).

Table 1 SHRIMP U-Pb isotopic data for zircons from monzogranites of the Zayu pluton of eastern Gangdese, Tibet[a)]

Spot	$^{206}Pb_c$ (%)	U (ppm)	Th (ppm)	Th/U	$^{206}Pb^*$ (ppm)	Isotopic ratios								$^{206}Pb/^{238}U$	±1σ
						$^{238}U/^{206}Pb^*$	±1σ	$^{207}Pb^*/^{206}Pb^*$	±1σ	$^{207}Pb^*/^{235}U$	±1σ	$^{206}Pb^*/^{238}U$	±1σ		
CY1-01, monzogranite, 13 spots (without spot 3), weighted mean age: 129.1 ± 1.6 Ma, MSWD = 1.9															
CY1-01-1.1	1.4	622	276	0.46	10.6	50.94	0.66	0.0449	0.0031	0.1216	0.0084	0.01963	0.00026	125.3	1.6
CY1-01-2.1	3.01	255	286	1.16	4.54	49.67	0.84	0.0472	0.0080	0.1310	0.0223	0.02013	0.00034	128.5	2.2
CY1-01-3.1	4.15	26	21	0.84	4.16	5.59	0.12	0.0657	0.0099	1.6200	0.2430	0.17900	0.00394	1062	22
CY1-01-4.1	1.69	740	354	0.49	13.1	49.31	0.64	0.0419	0.0035	0.1172	0.0098	0.02028	0.00026	129.4	1.7
CY1-01-5.1	3.79	197	174	0.91	3.65	48.20	1.40	0.0650	0.0088	0.1870	0.0239	0.02076	0.00034	132.4	3.8
CY1-01-6.1	2.1	346	233	0.7	6.15	49.28	0.74	0.0468	0.0056	0.1310	0.0170	0.02029	0.00030	129.5	1.9
CY1-01-7.1	0.94	891	284	0.33	15.7	49.18	0.59	0.0473	0.0025	0.1326	0.0070	0.02033	0.00024	129.8	1.6
CY1-01-8.1	3.17	268	226	0.87	4.74	50.22	0.85	0.0423	0.0080	0.1160	0.0220	0.01991	0.00034	127.1	2.1
CY1-01-9.1	2.65	250	234	0.97	4.46	49.53	0.84	0.0500	0.0080	0.1390	0.0222	0.02019	0.00034	128.9	2.2
CY1-01-10.1	0.41	1620	738	0.47	29	48.22	0.58	0.0490	0.0013	0.1400	0.0042	0.02074	0.00025	132.3	1.6
CY1-01-11.1	0.58	1493	624	0.43	27	47.74	0.57	0.0483	0.0015	0.1394	0.0046	0.02095	0.00025	133.6	1.6
CY1-01-12.1	1.75	478	327	0.71	8.4	49.77	0.70	0.0442	0.0040	0.1220	0.0111	0.02009	0.00028	128.2	1.7
CY1-01-13.1	2.81	378	281	0.77	6.63	50.42	0.76	0.0427	0.0060	0.1170	0.0164	0.01983	0.00030	126.6	1.9
CY1-01-14.1	4.34	273	194	0.73	4.88	50.35	0.86	0.0382	0.0088	0.1040	0.0239	0.01986	0.00034	126.8	2.2
CY6-1, monzogranite, 9 spots (without spot 1, 9, 10, 11), weighted mean age: 128.5 ± 3.1 Ma, MSWD = 4.5															
CY6-1-1.1	0.44	1788	1671	0.97	34.9	44.19	0.53	0.0465	0.0011	0.1452	0.0038	0.02263	0.00027	144.3	1.7
CY6-1-2.1	1.41	297	249	0.87	5.35	48.35	0.68	0.0547	0.0024	0.1561	0.0072	0.02068	0.00029	132.0	1.8
CY6-1-3.1	0.99	599	236	0.41	10.7	48.50	0.63	0.0481	0.0031	0.1368	0.0090	0.02062	0.00027	131.6	1.7
CY6-1-4.1	2.53	204	164	0.83	3.59	50.09	0.95	0.0448	0.0094	0.1230	0.0258	0.01996	0.00038	127.4	2.3
CY6-1-5.1	4.1	254	169	0.69	4.33	52.58	0.89	0.0408	0.0078	0.1070	0.0203	0.01902	0.00032	121.5	2.0
CY6-1-6.1	1.49	717	502	0.72	12.6	49.67	0.65	0.0460	0.0035	0.1276	0.0098	0.02013	0.00026	128.5	1.7
CY6-1-7.1	2.79	337	353	1.08	5.84	50.94	0.82	0.0477	0.0076	0.1290	0.0206	0.01963	0.00031	125.3	2.0
CY6-1-8.1	1.7	258	214	0.86	4.72	47.81	0.76	0.0570	0.0063	0.1640	0.0180	0.02092	0.00033	133.4	2.2
CY6-1-9.1	0.87	363	317	0.9	5.91	53.16	0.74	0.0551	0.0029	0.1429	0.0077	0.01881	0.00026	120.1	1.6
CY6-1-10.1	0.28	2603	726	0.29	50	44.88	0.54	0.0487	0.0008	0.1495	0.0030	0.02228	0.00027	142.1	1.6
CY6-1-11.1	1.17	844	654	0.8	15.8	46.50	0.60	0.0461	0.0028	0.1367	0.0083	0.02151	0.00028	137.2	1.7
CY6-1-12.1	0.65	425	363	0.88	7.6	48.34	0.68	0.0597	0.0041	0.1700	0.0119	0.02069	0.00029	132.0	1.9
CY6-1-13.1	2.23	413	386	0.97	7.05	51.40	0.77	0.0438	0.0057	0.1180	0.0153	0.01946	0.00029	124.2	1.8

a) $^{206}Pb_c$ (%) denotes the proportion of common ^{206}Pb in total measured $^{206}Pb^*$. $^{206}Pb^*$ (ppm) indicates radiogenic lead. Common Pb corrected using measured ^{204}Pb.

Table 2 Bulk-rock geochemical data of the Zayu pluton of eastern Gangdese, Tibet[a)]

	CY1-01	CY1-02	CY1-02R	CY1-1	CY2-1	CY3-1	CY4-1	CY6-1
XRF-major element (wt%)								
SiO_2	70.57	70.74	70.78	69.92	76.77	75.40	74.47	75.40
TiO_2	0.54	0.48	0.47	0.45	0.26	0.22	0.31	0.24
Al_2O_3	13.95	13.86	13.85	14.63	11.63	12.44	13.08	12.56
TFe_2O_3	3.43	3.14	3.14	3.04	2.03	1.92	2.32	1.65
MnO	0.05	0.04	0.04	0.04	0.02	0.03	0.03	0.02
MgO	0.93	0.77	0.76	0.67	0.37	0.23	0.44	0.31
CaO	2.12	1.75	1.75	1.89	1.25	0.91	1.50	1.35
Na_2O	2.57	2.55	2.55	3.24	2.69	2.78	2.92	2.72
K_2O	5.05	5.73	5.72	5.39	4.37	5.62	4.57	4.84
P_2O_5	0.12	0.10	0.10	0.11	0.06	0.05	0.07	0.06
LOI	0.20	0.41	0.37	0.17	0.14	0.25	0.22	0.94
Total	99.53	99.57	99.53	99.55	99.59	99.85	99.93	100.09
K_2O/Na_2O	1.96	2.25	2.24	1.66	1.62	2.02	1.57	1.78
FeO*/MgO	3.3	3.7	3.7	4.1	4.9	7.5	4.7	4.8
A/CNK	1.03	1.02	1.02	1.00	1.02	1.01	1.05	1.03
A/NK	1.44	1.33	1.33	1.31	1.27	1.17	1.34	1.29
Normative CIPW (%)								
Quartz	30.35	29.15	29.24	25.43	41.2	35.4	36.03	37.93
Anorthite	9.82	8.11	8.11	8.73	5.85	4.21	7.01	6.37
Albite	21.94	21.8	21.8	27.63	22.92	23.64	24.81	23.24
Orthoclase	30.11	34.21	34.15	32.11	26	33.38	27.12	28.88
Corundum	0.69	0.53	0.53	0.29	0.35	0.25	0.77	0.54
Diopside	0	0	0	0	0	0	0	0
Hypersthene	3.71	3.07	3.06	2.74	1.84	1.34	2.09	1.44
Ilmenite	1.03	0.92	0.9	0.86	0.5	0.42	0.59	0.46
Magnetite	2.07	1.98	1.98	1.95	1.21	1.23	1.4	1.01
Apatite	0.29	0.24	0.24	0.27	0.15	0.12	0.17	0.15
Total	100.01	100.01	100.01	100.01	100.01	100	100.01	100.01
ICP-MS-trace element (ppm)								
Be	2.34	3.35	3.50	2.86	2.59	4.23	2.39	2.71
Sc	7.42	8.56	8.48	8.35	3.82	3.90	4.53	3.05
V	40.7	32.7	33.3	29.0	17.2	7.80	20.9	14.3
Cr	10.5	8.25	8.19	7.49	3.70	2.28	4.19	3.44
Co	5.86	4.52	4.53	4.57	2.62	1.71	3.20	2.21
Ni	4.33	3.59	3.52	3.69	1.95	1.22	2.42	1.86
Cu	4.70	4.32	6.34	6.31	2.39	2.92	3.23	2.44
Zn	46.6	47.8	49.9	41.1	31.8	32.2	34.0	25.3
Ga	18.6	19.0	19.1	19.3	15.7	18.9	17.9	16.1
Rb	203	275	269	248	203	312	191	189
Sr	144	108	109	101	58.5	51.7	77.7	73.3
Y	30.3	48.7	46.4	51.2	34.1	53.6	27.1	24.6
Zr	230	191	240	216	157	221	212	226
Nb	13.4	14.3	13.9	15.0	9.23	12.1	9.38	8.95
Cs	9.82	12.5	12.5	6.18	6.50	7.09	5.49	6.89
Ba	694	498	489	605	249	254	338	382
La	67.1	77.4	67.6	49.2	46.3	76.1	66.4	55.2
Ce	126	149	130	98.9	89.0	148	124	105
Pr	12.9	15.7	13.8	11.0	9.12	15.4	12.5	10.5
Nd	47.8	59.0	52.1	43.8	33.7	55.8	44.9	37.6
Sm	8.21	11.2	10.2	9.86	6.42	10.6	7.43	6.43
Eu	1.33	1.11	1.10	1.02	0.74	0.89	0.93	0.87
Gd	6.92	10.0	9.16	9.35	5.73	9.35	6.17	5.48
Tb	1.01	1.57	1.48	1.62	0.91	1.53	0.90	0.80

(*To be continued on the next page*)

(*Continued*)

	CY1-01	CY1-02	CY1-02R	CY1-1	CY2-1	CY3-1	CY4-1	CY6-1
Dy	5.55	9.18	8.62	9.61	5.45	9.05	4.87	4.41
Ho	1.06	1.75	1.64	1.86	1.12	1.84	0.94	0.86
Er	2.98	4.78	4.57	5.03	3.39	5.36	2.64	2.45
Tm	0.44	0.70	0.66	0.73	0.53	0.82	0.39	0.37
Yb	2.67	4.10	3.96	4.23	3.34	5.09	2.45	2.26
Lu	0.38	0.56	0.55	0.58	0.48	0.71	0.35	0.34
Hf	5.82	5.15	6.45	5.80	4.52	6.18	5.55	6.22
Ta	1.15	1.25	1.18	1.20	1.46	1.46	0.84	0.77
Pb	30.6	35.4	34.5	33.0	27.4	42.9	26.5	29.1
Th	24.4	85.9	48.9	27.2	73.6	55.8	33.3	34.3
U	2.87	8.66	5.45	2.57	7.36	8.25	2.51	3.94
Sr-Nd isotope compositions								
$(^{87}Rb/^{86}Sr)_m$	4.0862			7.0855		17.4673	7.1293	7.4785
$(^{87}Sr/^{86}Sr)_m$	0.725460			0.730375		0.744253	0.729346	0.730475
$\pm 2\sigma$	0.000014			0.000012		0.000010	0.000014	0.000011
$(^{87}Sr/^{86}Sr)_i$	0.71791			0.71728		0.71198	0.71617	0.71666
$(^{147}Sm/^{144}Nd)_m$	0.1037			0.1361		0.1153	0.1001	0.1033
$(^{143}Nd/^{144}Nd)_m$	0.511999			0.512115		0.512177	0.512081	0.512072
$\pm 2\sigma$	0.000005			0.000008		0.000006	0.000005	0.000008
$\varepsilon_{Nd}(t)$	−10.9			−9.2		−7.6	−9.3	−9.5
$(^{143}Nd/^{144}Nd)_i$	0.51191			0.51200		0.51208	0.51200	0.51198
T_{DM} (Ga)	1.6			2.0		1.5	1.4	1.5
T_{DM2} (Ga)	1.8			1.7		1.5	1.7	1.7
T_{Zr} (℃)	815	798	818	804	789	816	815	821

a) LOI=loss on ignition. m = measured values. A/CNK = molecular $Al_2O_3/(CaO + Na_2O + K_2O)$, A/NK = molecular $Al_2O_3/(Na_2O + K_2O)$. Corrected formula as follows: $(^{87}Sr/^{86}Sr)_i = (^{87}Sr/^{86}Sr)_{sample} + {}^{87}Rb/^{86}Sr\ (e^{\lambda t} - 1)$, $\lambda = 1.42 \times 10^{-11}\ a^{-1}$; $(^{143}Nd/^{144}Nd)_i = (^{143}Nd/^{144}Nd)_{sample} + (^{147}Sm/^{144}Nd)_m \times (e^{\lambda t} - 1)$, $\varepsilon_{Nd}(t) = [(^{143}Nd/^{144}Nd)_{sample} / (^{143}Nd/^{144}Nd)_{CHUR}(t) - 1] \times 10^4$, $(^{143}Nd/^{144}Nd)_{CHUR}(t) = 0.512638 - 0.1967 \times (e^{\lambda t} - 1)$. $T_{DM} = 1/\lambda \times \ln \{1 + [((^{143}Nd/^{144}Nd)_{sample} - 0.51315)/((^{147}Sm/^{144}Nd)_{sample} - 0.21317)]\}$, $\lambda_{Sm\text{-}Nd} = 6.54 \times 10^{-12}\ a^{-1}$; T_{DM2} is the two-stage Nd depleted-mantle model age calculated using the same assumption formulation as ref. [40]. Zircon saturation temperature (T_{Zr}) is calculated using the assumption formulation as ref. [41].

Table 3 Hf isotopic data for zircons from a monzogranite sample (CY1-01) of the Zayu pluton of eastern Gangdese, Tibet[a)]

No.	Age (Ma)	$^{176}Yb/^{177}Hf$	$^{176}Lu/^{177}Hf$	$^{176}Hf/^{177}Hf$	$\pm 2\sigma$	$(^{176}Hf/^{177}Hf)_t$	$\varepsilon_{Hf}(0)$	$\varepsilon_{Hf}(t)$	T_{DM} (Ma)	T_{DM}^{C} (Ma)	$f_{Lu/Hf}$
01	125	0.026850	0.000870	0.282599	0.000019	0.282597	−6.1	−3.5	922	1403	−0.97
02	129	0.026183	0.000846	0.282613	0.000018	0.282611	−5.6	−2.9	902	1369	−0.97
03	129	0.046795	0.001516	0.282456	0.000017	0.282453	−11.2	−8.5	1140	1723	−0.95
04	130	0.027948	0.000812	0.282504	0.000013	0.282502	−9.5	−6.7	1052	1611	−0.98
05	130	0.024409	0.000714	0.282569	0.000014	0.282567	−7.2	−4.4	959	1465	−0.98
06	132	0.023860	0.000708	0.282533	0.000014	0.282531	−8.5	−5.6	1009	1545	−0.98
07	127	0.029589	0.000870	0.282602	0.000015	0.282600	−6.0	−3.3	917	1394	−0.97
08	129	0.036451	0.001041	0.282505	0.000013	0.282503	−9.4	−6.7	1057	1611	−0.97
09	132	0.095769	0.002740	0.282404	0.000014	0.282397	−13.0	−10.4	1256	1845	−0.92
10	134	0.040347	0.001168	0.282520	0.000014	0.282517	−8.9	−6.1	1041	1577	−0.96
11	128	0.030036	0.000890	0.282342	0.000016	0.282340	−15.2	−12.5	1281	1976	−0.97
12	127	0.029409	0.000844	0.282488	0.000014	0.282486	−10.0	−7.3	1075	1649	−0.97
13	127	0.025675	0.000742	0.282544	0.000016	0.282542	−8.1	−5.4	995	1525	−0.98

a) $\varepsilon_{Hf}(t) = 10000 \times \{[(^{176}Hf/^{177}Hf)_S - (^{176}Lu/^{177}Hf)_S \times (e^{\lambda t} - 1)]/[(^{176}Hf/^{177}Hf)_{CHUR,0} - (^{176}Lu/^{177}Hf)_{CHUR} \times (e^{\lambda t} - 1)] - 1\}$. $T_{DM} = 1/\lambda \times \ln\{1 + [(^{176}Hf/^{177}Hf)_S - (^{176}Hf/^{177}Hf)_{DM}]/[(^{176}Lu/^{177}Hf)_S - (^{176}Lu/^{177}Hf)_{DM}]\}$. $T_{DM}^{C} = T_{DM} - (T_{DM} - t) \times [(f_{cc} - f_s)/(f_{cc} - f_{DM})]$. $f_{Lu/Hf} = (^{176}Lu/^{177}Hf)_S/(^{176}Lu/^{177}Hf)_{CHUR} - 1$, where, $\lambda = 1.867 \times 10^{-11}\ a^{-1}$ [44]; $(^{176}Lu/^{177}Hf)_S$ and $(^{176}Hf/^{177}Hf)_S$ are the measured values of the samples; $(^{176}Lu/^{177}Hf)_{CHUR} = 0.0332$, $(^{176}Hf/^{177}Hf)_{CHUR,0} = 0.282772$[46]; $(^{176}Lu/^{177}Hf)_{DM} = 0.0384$, $(^{176}Hf/^{177}Hf)_{DM} = 0.28325$[47]; $(^{176}Lu/^{177}Hf)_{mean\ crust} = 0.015$; $f_{cc} = [(^{176}Lu/^{177}Hf)_{mean\ crust}/(^{176}Lu/^{177}Hf)_{CHUR}] - 1$; $f_s = f_{Lu/Hf}$; $f_{DM} = [(^{176}Lu/^{177}Hf)_{DM}/(^{176}Lu/^{177}Hf)_{CHUR}] - 1$; t = crystallization time of zircon.

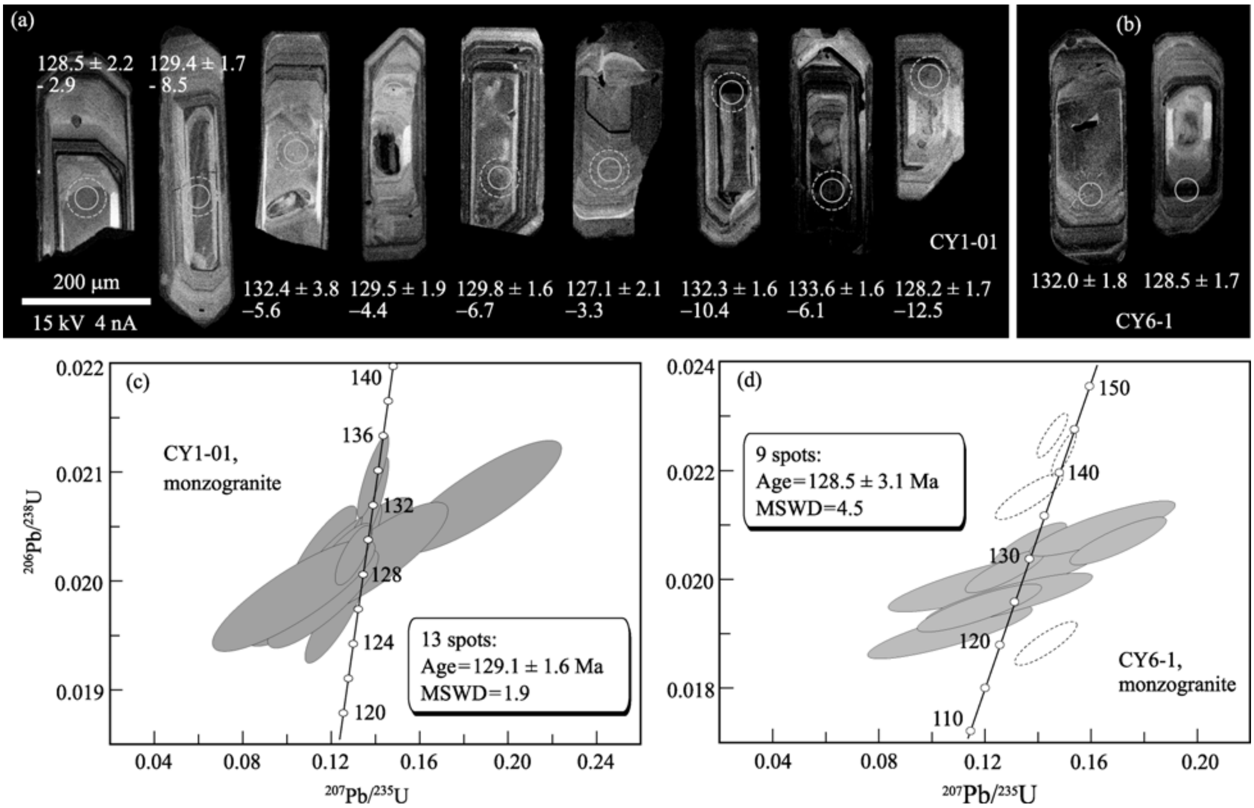

Figure 2 Cathodoluminescence (CL) images of representative zircon ((a) and (b)) and concordia diagrams ((c) and (d)) for zircons from the Zayu pluton. Solid and dashed circles indicate the locations of SHRIMP U-Pb dating and LA-ICPMS Hf analyses, respectively.

3.2 Bulk-rock geochemistry

The Zayu pluton samples are characterized by high SiO_2 (69.9%—76.8%), K_2O (4.4%—5.7%), K_2O/Na_2O ratios (1.57—2.25) and low P_2O_5 (0.05%—0.12%), and are of monzogranite to syenogranite composition (Figure 3(a)). Negative correlations are presented between Al_2O_3, P_2O_5 and SiO_2 (Figure 3(b) and (c)). The differentiation index of the Zayu pluton samples ranges from 82 to 92, comparable to that of the highly fractionated I-type granites (82—94) in Fogang, South China[48]. The A/CNK values (1.00—1.05), presence of minor normative corundum (0.25%—0.77%), and absence of normative diopside of the Zayu pluton samples are consistent with them being metaluminous to slightly peraluminous granites.

The Zayu pluton samples clearly display negative Eu anomalies (δEu = 0.27—0.54) and are variably enriched in light rare earth elements (REEs) ((La/Yb) = 8.3—19.4) (Figure 4(a)). In primitive mantle-normalized spidergram, the Zayu pluton samples are enriched in large-ion lithophile elements (LILEs; e.g., U, Th, Rb, and K), light REEs and Pb, and clearly depleted in high field strength elements (e.g., Nb, Ta, Ti, and to a much lesser extent Zr and Hf), and elements reflecting plagioclase (e.g., Sr and Ba) and apatite (P) fractionation relative to LILEs (Figure 4(b)).

The Zayu pluton samples have higher $\varepsilon_{Nd}(t)$ values of −10.9—−7.6 and lower $(^{87}Sr/^{86}Sr)_i$ ratios of 0.7120—0.7179 than those of the Early Jurassic Ningzhong muscovite monzogranites that have been considered as representing melts derived from mature continental crust of the Gangdese Retro-arc Uplift Belt ($\varepsilon_{Nd}(t)$ = −14.4—−12.0, $(^{87}Sr/^{86}Sr)_i$ = 0.7714—0.8643[52], corrected to 130 Ma) (Figure 5). The Zayu pluton samples have two-stage Nd model ages of 1.5—1.8 Ga.

3.3 Zircon Hf isotope

The 13 analyses on zircons give $^{176}Yb/^{177}Hf$ and $^{176}Lu/^{177}Hf$ values of 0.023860—0.095769 and 0.000708—0.002740, respectively (Table 3). The $^{176}Lu/^{177}Hf$ values are much lower or closer than 0.002, indicating a minor accumulation of radiogenic Hf. This means that the

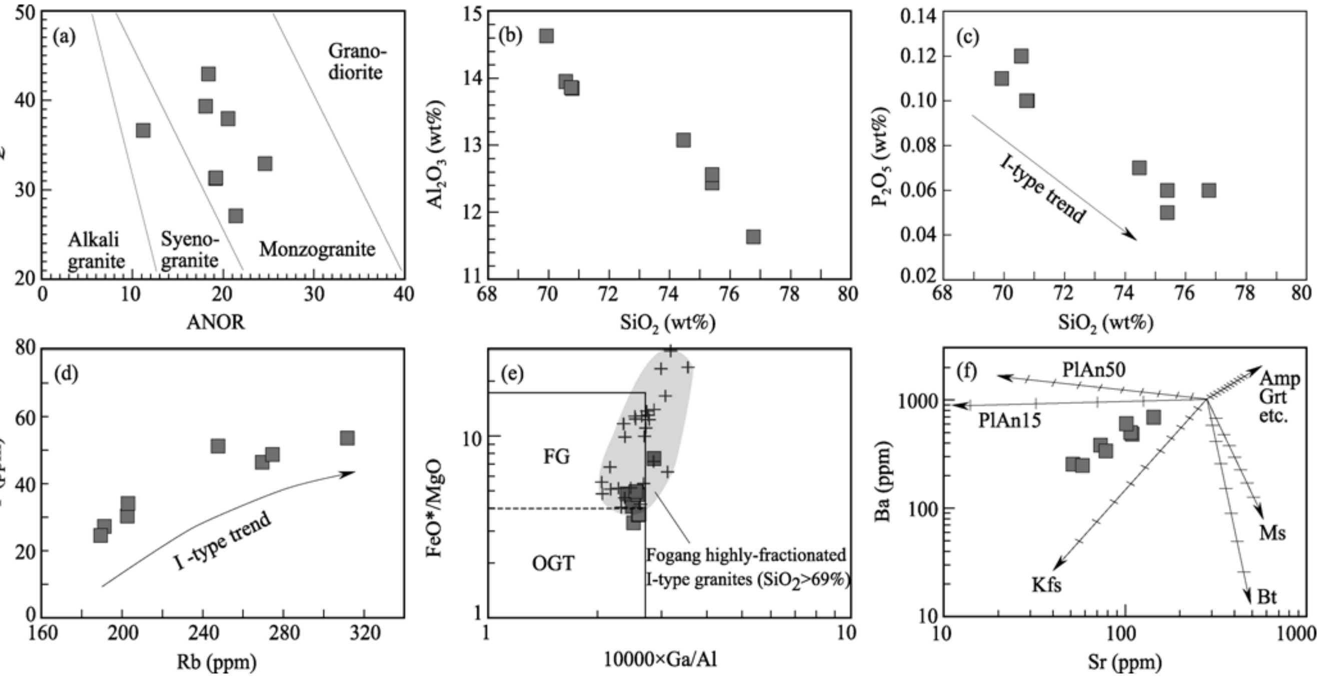

Figure 3 Selected geochemical diagrams of the Zayu pluton. (a) Q′-ANOR normative composition diagram[49] of the Zayu pluton: Q′ = Q × 100/(Q + Or + Ab + An), ANOR = An × 100/(Or + An); (b)—(d) scattered plots; (e) FeO*/MgO vs. 10000 × Ga/Al classification diagram[50]: FG = Fractionated M-, I- and S-type granites, OGT = unfractionated M-, I- and S-type granites; highly fractionated I-type granites (82—94) in Fogang, South China[48]; (f) Ba vs. Sr plot[48]: vectors represent 50% fractionation crystallization of the main rock-forming minerals. Pl_{An50}, plagioclase (An = 50); Pl_{An10}, plagioclase (An = 10); Kfs, K-feldspar; Amp, amphibole; Grt, garnet; Ms, muscovite; Bt, biotite.

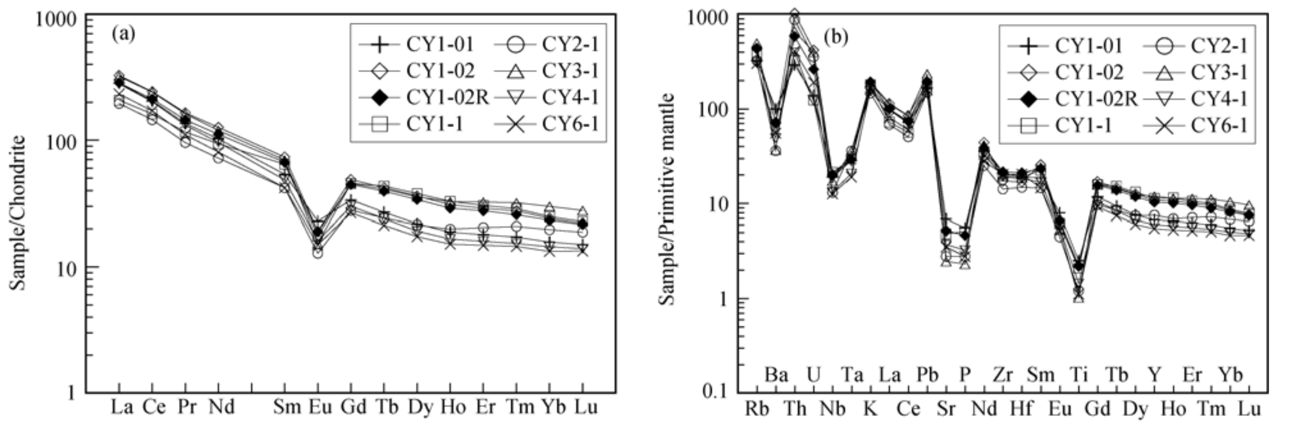

Figure 4 Chondrite-normalized REE and primitive-mantle-normalized trace element patterns for the Zayu pluton. Data for normalization and plotting are from ref. [51].

$^{176}Hf/^{177}Hf$ ratios of the melt from which zircons crystallized can be represented by the initial $^{176}Hf/^{177}Hf$ ratios[54]. The 13 analyses give $\varepsilon_{Hf}(t)$ values of −12.5—−2.9 with a large variation of up to 9.6 epsilon units (Figure 6(a)), significantly exceeding the external errors during the analysis. Therefore, the zircon Hf isotopic-compositions of this sample are heterogeneous. Hence, this sample gives a wide range of zircon Hf isotope crustal model ages (T_{DM}^{C}) of 1.4—2.0 Ga (Figure 6(b)), similar to the two-stage Nd model ages.

4 Discussions

4.1 Comparison of the Zayu pluton with Early Cretaceous magmatic rocks in other locations in the Gangdese

Existing data indicated that the Early Cretaceous magmatism in the southern Gangdese took place during

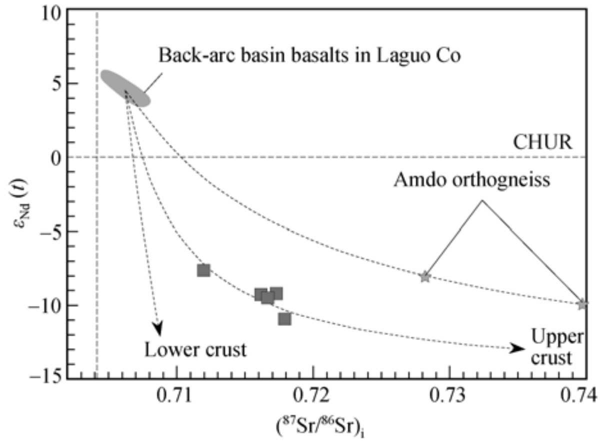

Figure 5 $\varepsilon_{Nd}(t)$ vs. $(^{87}Sr/^{86}Sr)_i$ diagram of the Zayu pluton. Back-arc basin basalts in Laguo Co (Bao-Di Wang, unpublished data) are assumed to represent isotopically the composition of mantle-derived magmas above subduction zone: $(^{87}Sr/^{86}Sr)_i$ = 0.70634, $\varepsilon_{Nd}(t)$ = 4.5, Sr = 196 ppm, Nd = 4.5 ppm (mean value of five samples); the Amdo orthogneiss[12] is assumed to represent isotopically the intracrustal metamorphosed mafic to intermediate igneous rocks: $(^{87}Sr/^{86}Sr)_i$ = 0.74001, $\varepsilon_{Nd}(t)$ = −10, Sr = 282 ppm[53], Nd = 22.2 ppm; the Ningzhong strongly peraluminous granites[52] are considered as representing melts derived from mature continental crust of the Gangdese: $(^{87}Sr/^{86}Sr)_i$ = 0.77139, $\varepsilon_{Nd}(t)$ = −14.3, Sr = 31.7 ppm, Nd= 12.6 ppm. Note that Sr and Nd isotopic data are all corrected to 130 Ma.

137—103 Ma, with positive bulk-rock $\varepsilon_{Nd}(t)$ values and zircon $\varepsilon_{Hf}(t)$ values, corresponding to Phanerozoic crustal model ages1),[31,33,55]. In the Gangdese Retro-arc Uplift Belt and middle Gangdese, the Early Cretaceous magmatism persisted from 143 to 102 Ma, and at ~130 Ma the magmatism synchronously occurred along a ~800 km long E-W belt from Xungba, via Coqen, Eyang, and to Zagong (Figure 7(a)). These rocks are dominated by negative $\varepsilon_{Hf}(t)$ values (−14.2—+3.4), corresponding to Paleoproterozoic-early Mesoproterozoic crustal model ages (0.8—2.1 Ga) with a peak at about 1.6 Ga (Figure 7(b))1),2). In the northern Gangdese, currently available data suggest that the Early Cretaceous magmatism occurred mostly between 124 and 109 Ma (Figure 7(a)), which are dominated by positive $\varepsilon_{Hf}(t)$ values (−1.1—+10.1), corresponding to crustal model ages of 0.5—1.3 Ga, with two peaks at 1.1 Ga and 0.7 Ga (Figure 7(b))1).

In the Zayu pluton of the eastern Gangdese, zircon SHRIMP U-Pb age dates (~129 Ma) of the two samples obtained in this study are identical within error to the zircon LA-ICPMS U-Pb age dates (133—130 Ma)[33] obtained in other parts of the Zayu pluton (Figure 1(b)). In addition, zircon LA-ICPMS U-Pb age dates of 130—109 Ma[32,33,35] are recently reported in the granitoids from the Bomi-Rawu-Baxoi areas of eastern Gangdese (Figure 7(a)). All these zircon U-Pb age dates suggest that the Early Cretaceous granitoids are almost synchronously emplaced during 133—109 Ma in eastern Gangdese (Figure 7(a)). Importantly, data obtained in this study and in the literature[32,33,35] suggest that these granitoids are characterized by dominantly negative $\varepsilon_{Hf}(t)$ values (−15.1—+5.0) and ancient crustal model ages of 0.9—2.1 Ga with a peak at about 1.7 Ga (Figure 7(b)).

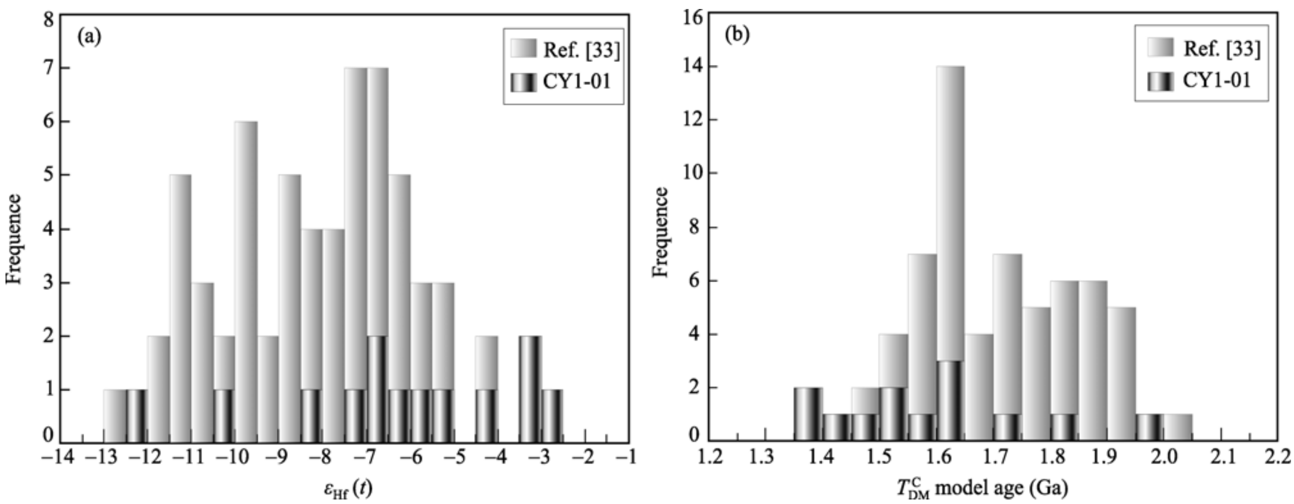

Figure 6 Histograms of $\varepsilon_{Hf}(t)$ values and zircon Hf isotope crustal model ages (T_{DM}^{C}) of the Zayu pluton.

1) see 1) on page 1224.
2) see 2) on page 1224.

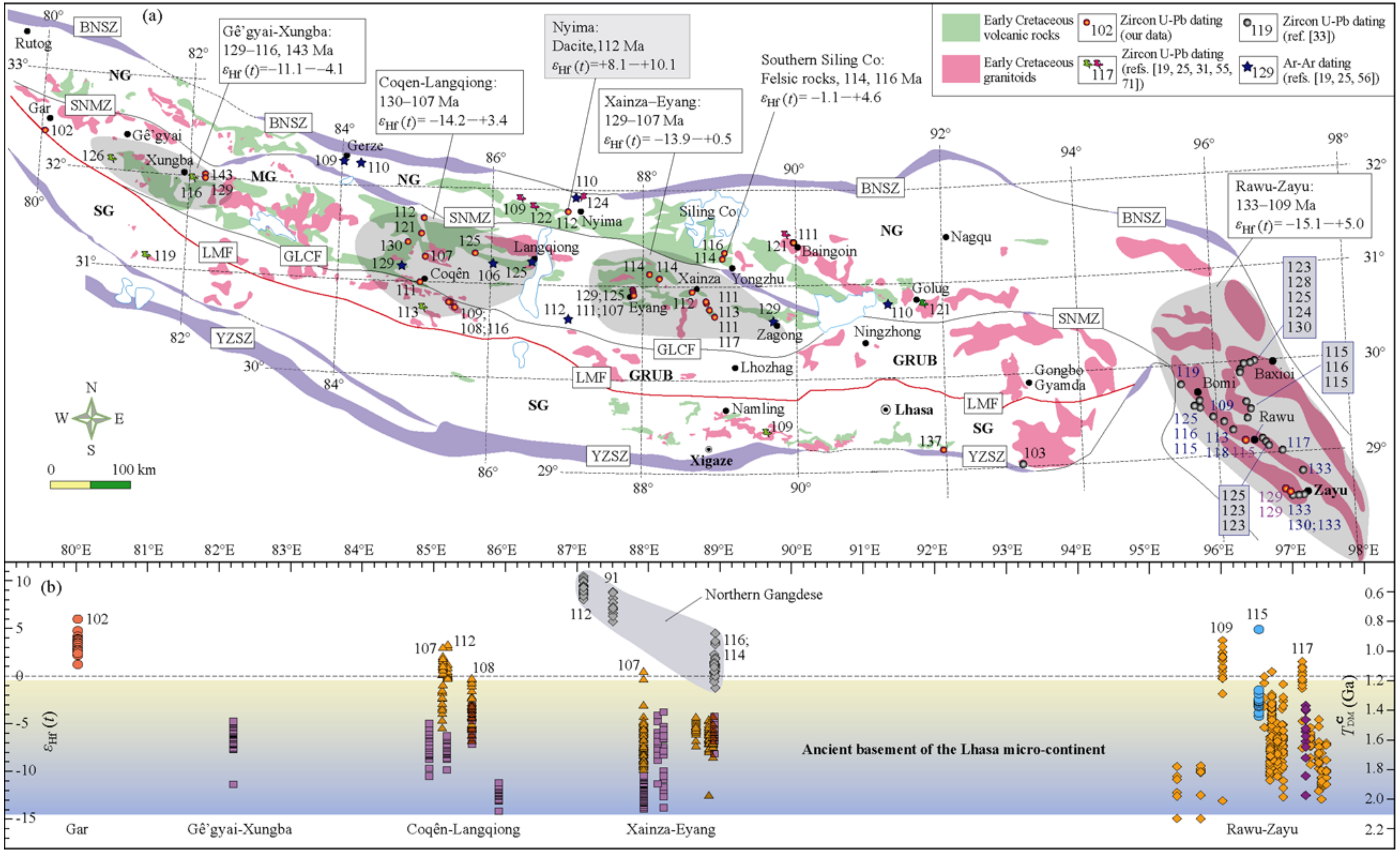

Figure 7 Spatial variations of zircon U-Pb age dates and Hf isotopic compositions of the Early Cretaceous magmatic rocks in the Middle and Northern Gangdese, Tibet.

These observations indicate that the Early Cretaceous granitoids in the Bomi-Rawu-Baxoi/Zayu areas of the eastern Gangdese are comparable with the contemporaneous granitoids in the middle Gangdese in terms of their emplacement ages (Figure 7(a)), zircon Hf isotopic compositions, and crustal model ages (Figure 7(b)). This means that the Early Cretaceous granitoids in the eastern Gangdese represent the eastward extension of the contemporaneous magmatism in the middle Gangdese.

Available zircon Hf isotopic data indicate major stages of continental crust growth in the middle Gangdese from the Paleoproterozoic to early Mesoproterozoic1),2). Because zircon Hf model ages are calculated from $\varepsilon_{\mathrm{Hf}}(t)$, and because crust-mantle interaction is inevitable (see below), the measured $\varepsilon_{\mathrm{Hf}}(t)$ values represent mixing between mantle-derived (large positive $\varepsilon_{\mathrm{Hf}}(t)$) and ancient crust-derived (large negative $\varepsilon_{\mathrm{Hf}}(t)$) materials. Hence, the $\varepsilon_{\mathrm{Hf}}(t)$ for the reworked crust should be more negative and the "crustal" model age should be even older. Therefore, the continental crust of the middle Gangdese should be formed before the Paleoproterozoic, which is comparable to the Archean crustal growth of the Gangdese Retro-arc Uplift Belt1). This is in contrast to the northern Gangdese that is dominated by Mesoproterozoic to Neoproterozoic juvenile materials and the southern Gangdese that is dominated by Phanerozoic juvenile materials. Therefore, Zhu et al.1),2) proposed that the middle Gangdese and Gangdese Retro-arc Uplift Belt (i.e., the central Lhasa Terrane) is effectively an ~1000-km-long and ~100-km-wide micro-continental block with ancient basement (i.e., the Lhasa micro-continental block) Although the zircon Hf isotopic data from the Gongbo gyamda-Golug-Nagqu areas are yet unavailable (Figure 7(a) and (b)), it is inferred from the Early Cretaceous strongly peraluminous granite in the Golug area (121 Ma)[57] and data obtained in this study and in the literature that the Lhasa micro-continental block with ancient basement may have extended eastward to the Rawu-Baxoi-Zayu areas with a distance up to 2000 km (Figure 7(b)).

4.2 Petrogenetic type

As discussed above, the Zayu pluton in the eastern Gangdese is comparable to the contemporaneous magmatic rocks in the middle Gangdese. Previous studies interpreted the Early Cretaceous granitoids in the Middle and northern Gangdese as the products of crustal anatexis in response to crustal thickening related to the Lhasa-Qiangtang collision[11−13,23]. Similar interpretation is also proposed for the generation of the Early Cretaceous granitoids in the Baxoi-Rawu-Zayu areas of eastern Gangdese[33]. Therefore, an effective recognition of the petrogenetic type of the Early Cretaceous granitoids in Zayu area is crucial for identifying their tectonic settings.

The absence of amphibole, together with the high SiO_2 (up to 77%), total alkali ($K_2O + Na_2O$ = 7.1%−8.6%) and FeO^*/MgO ratios (3.3−7.5), suggest the Zayu pluton samples experienced significant magmatic differentiation. Experimental results[58] indicate that apatite solubility is very low in metaluminous and slightly peraluminous melts (I-type), and decreases with increasing SiO_2 content during magmatic differentiation, while an inverse trend of apatite solubility occurs in peraluminous melts (S-type). Such different behaviors of apatite in I- and S-type granitic melts are successfully used to distinguish I- and S-type granitoids[48,59−62]. Data obtained in this study indicate that the Zayu pluton samples are slightly peraluminous (A/CNK < 1.1), very low P_2O_5 (<0.12%) that decreases with increasing SiO_2 content (Figure 3(c)). These features are consistent with the differentiation trend of I-type granitic magmas. Such a trend is also supported by the positive correlation between yttrium and rubidium (Figure 3(d)). This is because behaviors of Y and other heavy REEs are controlled by garnet that is characteristic in S-type granite magma (Al-rich melts), and yttrium-rich minerals will not crystallize from metaluminous I-type magma during early stage of magmatic differentiation, consequently resulting in a high Y abundance and a positive correlation between Y and Rb in differentiated I-type granites[62]. In addition, the Zayu pluton samples have limited 10000×Ga/Al (2.4−2.9) but are high in FeO*/MgO (3.3−7.5) similar to those of the highly fractionated Fogang I-type granites in South China[48], and the majority of the Zayu pluton samples are plotted into the highly fractionated calc-alkaline granite field (Figure 3(e))[50]. Thus, the Zayu pluton samples we studied are of highly fractionated I-type granites. This recognition,

1) see 1) on page 1224.
2) see 2) on page 1224.

together with the presence of the contemporaneous highly fractionated S-type granites identified by Lin[36] in the granitoids of the Zayu area, suggest that the contemporaneous highly fractionated I- and S-type granitoids are both present in the Zayu pluton.

4.3 Petrogenesis

The data obtained in this study and in the literature indicate that the Zayu pluton samples are characterized by negative zircon $\varepsilon_{\mathrm{Hf}}(t)$ values (Figure 6(a)), ancient crustal model ages (1.4－2.0 Ga) (Figure 6(b)), and negative bulk-rock $\varepsilon_{\mathrm{Nd}}(t)$ values (Table 3). It follows that these rocks were derived from anatexis or remelting of ancient continental crust. However, it should be noted that samples we studied (up to 9.6-ε units) as well as samples collected from other parts of the Zayu pluton (up to 7.6-ε units)[33] all show zircon Hf isotopic heterogeneities (Figure 6(a)). Such a heterogeneity of zircon Hf isotopic composition within individual pluton requires open system processes, reflecting source compositional variation controlled parental melt compositional variation and complex magma chamber processes[63]. Because Hf isotope ratios of the melts parental to zircons are not modified due to processes of partial melting or fractional crystallization, and therefore the heterogeneity of zircon Hf isotope indicates mixing between more radiogenic (i.e., mantle-derived) and less radiogenic (crustal) end-members[64]. Thus, like the presence of heterogeneous zircon Hf isotopic compositions observed elsewhere in the world[45,48,63－66], the zircon Hf isotopic heterogeneity of the Zayu pluton is interpreted here as the result of mixing between mantle- and crust-derived magmas. This interpretation is also supported by the negative correlation of bulk-rock Sr and Nd isotopic data. As shown in Figure 5, by assuming (i) the Early Jurassic Ningzhong peraluminous granites[52] of the Gangdese Retro-arc Uplift Belt represent isotopically the composition of melts derived from anatexis of mature ancient crust within the Lhasa micro-continental block and (ii) the mantle-derived melts identified in the Zayu pluton are represented by the back-arc basin basalts in Laguo Co (Bao-Di Wang, unpublished data) in the Shiquan River-Nam Co Mélange Zone (SNMZ), it is suggested that the Sr and Nd isotopic compositions of the Zayu pluton can be explained by variable contributions from these two assumed end-members (Figure 5).

Previous studies suggested that I-type granites are derived from partial melting of intracrustal metamorphosed mafic to intermediate igneous rocks[67]. However, the most enriched $\varepsilon_{\mathrm{Nd}}(t)$ value (−10.9) of the Zayu pluton obtained in this study is lower than that of the Amdo orthogneiss ($\varepsilon_{\mathrm{Nd}}$(130 Ma) = −10－−8.1)[12] that can be considered as intracrustal igneous rocks of the Gangdese. In addition, five samples from the Zayu pluton are displaced from the mixing curve defined by the Amdo orthogneiss and the back-arc basin basalts in Laguo Co (Figure 5). These observations suggest that the Zayu pluton cannot be generated by mixing between intracrustal mafic igneous rock-derived magmas and mantle-derived magmas. Recent studies on zircon U-Pb age and zircon Hf and O isotope indicated that I-type granite can also be generated by the reworking of sedimentary materials that have been modified by mantle-like magmas[63] or the shift from S- to I-type granites can also be attributed to lesser amounts of sediment involved in crustal remelting[68]. As discussed earlier, the magma source region of the Zayu pluton is dominated by ancient crustal materials and the Zayu pluton reflects a variable extent of mixing with mantle-derived magmas. In this case, the I-type granites (with variable contributions of mantle-derived materials) observed in this study from the Zayu pluton can be interpreted as the results of mixing between ancient crustal material-derived melts and contributions of mantle-derived melts (relative to S-type granite that contains more crust-derived components).

Obviously, it is difficult to explain the bulk-rock geochemistry observed in the Zayu pluton solely by fractional crystallization of the hybrid melts with variable contributions of mantle-derived materials and predominant crust-derived components. The melts parental to the Zayu pluton must have experienced significant fractional crystallization, as indicated by the geochemical features of silica-rich, marked depletion in Ba, Nb, Ta, Sr, P, Ti, and Eu (Figure 4(b)). For example, depletions in Nb, Ta, and Ti generally demonstrate the separation of Ti-bearing phases (e.g., ilmenite and/or rutile). Strong P depletion suggests a fractionation of apatite. Plagioclase fractionation explains well the strong Eu and Sr (to a lesser extent for Ba depletion) (Figure 3(f)). Therefore, the Zayu pluton is most likely formed by strong fractional crystallization of a hybrid parental magma with both mantle-derived melt and melt of ancient crustal melting triggered by intrusion of mantle melts.

4.4 Discussions on geodynamic setting

As discussed above, extensive granitoids related to anatexis or remelting of ancient continental crust were emplaced at about 130 Ma in the Zayu area, eastern Gangdese. Continental crust materials would not melt unless there exist excess radioactive elements (e.g., K, U and Th) as heat source, which is generally associated with a thickened crust in a post-collisional setting (e.g., Miocene leucogranite in North Himalaya)[4,8]. Previous studies proposed that the crust of the middle and northern Gangdese was significantly shortened (>50%) prior to the India-Asia collision[25]. Such a crustal shortening (hence crustal thickening) was generally considered as one of the important observations for the interpretation that the Early Cretaceous S-type granitoids were associated with the remelting of thickened crust in a post-collisional setting[33]. However, it should be pointed out that such a proposed crustal shortening mainly occurred in the Late Cretaceous[18,19], significantly post-dating the anatexis or remelting of ancient continental crust in the middle Gangdese and the Zayu-Rawu-Baxoi areas of eastern Gangdese during the Early Cretaceous (at about 130 Ma)[33].

Zircon saturation temperature analysis[41] suggests that the temperature of the hybrid magma parental to the highly fractionated I-type Zayu granitoids (789－821℃) is identical to the Fogang granite in South China (728－840℃)[48] involving mantle-derived material in its generation, both of which are higher than those of the Miocene leucogranite in North Himalaya (667－769℃)[69] (Figure 8). Therefore, although no mafic rocks of ~130 Ma are yet reported in the Zayu area, zircon Hf isotopic data together with zircon saturation temperature of bulk-rocks suggest that mantle-derived materials must have played an important role in the generation of the Zayu pluton. In fact, the Early Cretaceous back-arc basin basalts in Asa, Yongzhu areas1),2) of the Shiquan River-Nam Co Mélange Zone (SNMZ) in the middle and northern Gangdese and the contemporaneous andesitic magmatism (~128 Ma[33]) in the Baxoi area of eastern Gangdese suggest the involvement of mantle-derived materials in the generation of the Early Cretaceous magmatism in the middle and northern Gangdese. The extensive zoned magmatism in the middle Gangdese synchronously occurred at about 130 Ma and persisted for a relatively long duration (lasted ~20 Ma) (Figure 7(a)). This situation can be readily explained by the scenario of seafloor subduction. This is because in subduction-related settings, mantle wedge basaltic magmas are hot enough to trigger the partial melting of crustal materials. Both mantle wedge basaltic melts and the induced crustal melts can mix to form hybrid melts parental to the highly fractionated I-type granitoids.

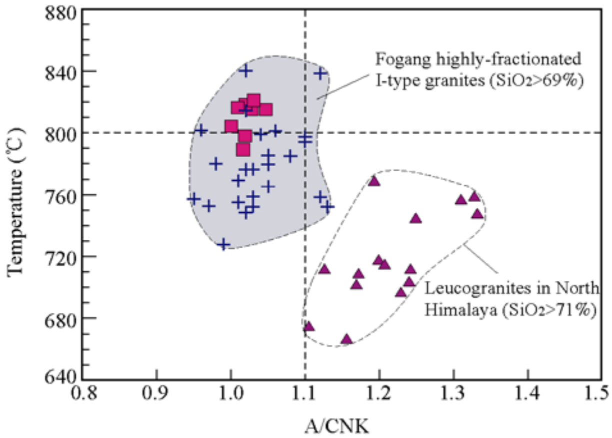

Figure 8 Plot of A/CNK vs. zircon saturation temperature of the Zayu pluton. Zircon saturation temperature was calculated using the method of ref. [41]; highly-fractionated I-type granites in Fogang, South China are from ref. [48]; leucogranites in North Himalaya are from ref. [69].

The Cretaceous magmatism in the middle and northern Gangdese was generally attributed to the low-angle or flab-slab northward subduction of the Neo-Tethyan Ocean seafloor[23,25,26,28,70,71]. However, this model needs revision because of the presence of the Early Cretaceous subduction-related magmatic rocks (137－109 Ma) recently identified in the southern Gangdese[30,31,55]. Studies on zircon U-Pb ages and zircon Hf isotopic composition of the Mesozoic igneous rocks sampled along a north-south traverse from Xigaze, via Namling, Lhozhag, and Xainza, to Siling Co/Nyima across the Gangdese (Figure 7(a)) suggested that the Gangdese Retro-arc Uplift Belt and middle Gangdese represent a micro-continental block with a width of ~100 km (i.e., the Lhasa micro-continental block)3). More recent studies

1) Qu Y G, Wang Y S, Duan J X, et al. 1:250000 geological report of Duoba with geological map, 2003. 106－127.

2) Xie G G, Zou A J, Yuan J Y, et al. 1:250000 geological report of Bangduo with geological map, 2003. 106－140.

3) see 1) on page 1224.

indicated that the Lhasa micro-continental block extends in E-W over 1000 km from Gar, via Xungba, and Coqen, to Xainza areas[1)] in the western and central parts of the Gangdese. The existence of the Lhasa micro-continental block and the negative gradient of zircon Hf isotopic compositions of the Mesozoic magmatic rocks from Nyima, via south Siling Co, to Xainza areas suggested that the Bangong-Nujiang Ocean must have a southward subduction zone for that ocean to finally close (i.e., Lhasa-Qiangtang collision)[1),2)]. This study indicates that the Lhasa micro-continental block with ancient basement extends eastward to the Rawu-Zayu areas of eastern Gangdese (Figure 7(b)). Therefore, the Early Cretaceous magmatism in the Rawu-Zayu areas can be attributed to the southward subduction of the Bangong-Nujiang Ocean seafloor (Figure 9) because the Cretaceous magmatism in the eastern Gangdese is comparable to that of the middle Gangdese. Under this framework, the parental magmas of the Early Cretaceous granitoids in Zayu area are controlled by the materials of the Lhasa micro-continental block itself and the relative contributions of mantle-derived magma. In other words, the so-called S-type granitoids (peraluminous magma) are mainly derived from the anatexis or remelting of the Lhasa micro-continental block itself (crustal thickening is not a prerequisite), whereas the so-called I-type granitoids (metaluminous magma) can be interpreted as resulting from the crust-derived melts that have mixed with mantle-derived melts.

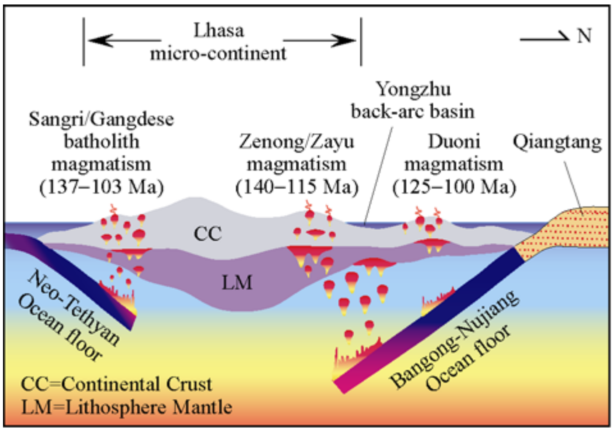

Figure 9 Geodynamic model for the Early Cretaceous magmatism in the Gangdese, Tibet (modified from 1)).

5 Conclusions

(1) Zircon U-Pb age dates indicate that the Zayu pluton is emplaced at about 130 Ma, coeval with the Early Cretaceous magmatic rocks in the middle Gangdese and other locations in the eastern Gangdese.

(2) The Zayu pluton samples are characterized by high Si, K, and low P, with A/CNK of 1.00—1.05, enriched in Rb, Th, U, and Pb, depleted in Ba, Nb, Ta, Sr, P, Ti, and Eu. They are highly fractionated metaluminous to slightly peraluminous I-type granitoids. The samples have higher $\varepsilon_{Nd}(t)$ (−10.9—−7.6) and lower $(^{86}Sr/^{87}Sr)_i$ (0.7120—0.7179) than those of the mature continental crust of the Gangdese. The Zayu pluton is characterized by heterogeneous zircon Hf isotopic compositions (−12.8—−2.9) with ancient crustal model ages (1.4—2.0 Ga).

(3) The Early Cretaceous granitoids in Zayu-Rawu-Baxoi areas in the eastern Gangdese represent the eastward extension of the Early Cretaceous magmatism in the middle Gangdese, and the Lhasa micro-continent block with ancient basement can be extended E-W for ~2000 km long.

(4) The Zayu pluton was most likely generated in a setting associated with the southward subduction of the Bangong-Nujiang ocean floor, where intrusion of mantle wedge basaltic magmas in the crust caused the anatexis of the latter, forming hybrid melts, which subsequently experienced high-degree fractional crystallization.

We thank Song Biao, Tao Hua from the Chinese Academy of Geological Sciences for helping with SHRIMP U-Pb dating; Liu Ye, Dai Mengning, and Zong Chunlei from the Northwest University for helping with bulk-rock geochemical analyses. We are indebted to Prof. Li Xianhua for inviting this contribution to the special volume of Science in China Series D: Earth Sciences. We also thank Profs. Chung Sun-Lin and Wu Fuyuan for constructive reviews.

1 Jahn B M, Wu F Y, Hong D W. Important crustal growth in the Phanerozoic: Isotopic evidence of granitoids from East-Central Asia. Proc Indian Acad Sci (Earth Planet Sci), 2000, 109: 5—20

2 Mo X X, Hou Z Q, Niu Y L, et al. Mantle contributions to crustal thickening during continental collision: Evidence from Cenozoic igneous rocks in southern Tibet. Lithos, 2007, 96: 225—242

1) see 2) on page 1224.
2) see 1) on page 1224.

3 Allègre C J, Ben Othman D. Nd-Sr isotopic relationship in granitoid rocks and continental crust development: A chemical approach to orogenesis. Nature, 1980, 286: 335－342

4 Sylvester P J. Postcollisional strongly peraluminous granites. Lithos, 1998, 45: 29－44

5 Patiño Douce A E. What do experiments tell us about the relative contributions of crust and mantle to the origin of granitic magmas? In: Castro A, Fernandez C, Vigneresse J L, eds. Understanding Granites: Integrating New and Classical Techniques. Geol Soc London Spec Publ, 1999, 168: 55－75

6 Clemens J D. S-type granitic magmas-petrogenetic issues, models and evidence. Earth Sci Rev, 2003, 61: 1－18

7 Healy B, Collins W J, Richards S W. A hybrid origin for Lachlan S-type granites: The Murrumbidgee Batholith example. Lithos, 2004, 78: 197－216

8 Niu Y L. Generation and evolution of basaltic magmas: Some basic concepts and a hypothesis for the origin of the Mesozoic-Cenozoic volcanism in eastern China. Geol J China Univ, 2005, 11(1): 9－46

9 Zhu D C, Mo X X, Niu Y L, et al. Zircon U-Pb dating and in-situ Hf isotopic analysis of Permian peraluminous granite in the Lhasa Terrane, southern Tibet: Implications for Permian collisional orogeny and paleogeography. Tectonophysics, 2009, 469: 48－60

10 Thompson A B. Some time-space relationships for crustal melting and granitic intrusion at various depths. In: Castro A, Fernandez C, Vigneresse J L, eds. Understanding Granites: Integrating New and Classical Techniques. Geol Soc, London Spe Publ, 1999, 168: 7－25

11 Harris N B W, Inger S, Xu R. Cretaceous plutonism in Central Tibet: An example of post-collision magmatism? J Volcanol Geotherm Res, 1990, 44: 21－32

12 Xu R H, Schärer U, Allègre C J. Magmatism and metamorphism in the Lhasa block (Tibet): A geochronological study. J Geol, 1985, 93: 41－57

13 Pearce J A, Mei H J. Volcanic rocks of the 1985 Tibet Geotraverse: Lhasa to Golmud. Philos Trans R Soc A-Math Phys Sci, 1988, 327: 169－201

14 Zhu D C, Pan G T, Chung S L, et al. SHRIMP zircon age and geochemical constraints on the origin of Early Jurassic volcanic rocks from the Yeba Formation, southern Gangdese in south Tibet. Int Geol Rev, 2008, 50: 442－471

15 Pan G T, Ding J, Wang L Q, et al. Geological map (1∶1500000) of Qinghai-Xizang (Tibetan) Plateau and Adjacent Areas (in Chinese). Chengdu: Chengdu Cartographic Publishing House, 2004

16 Zhu D C, Pan G T, Mo X X, et al. Late Jurassic-Early Cretaceous geodynamic setting in middle-northern Gangdese: New insights from volcanic rocks (in Chinese with English abstract). Acta Petrol Sin, 2006, 22(3): 534－546

17 Zhu D C, Pan G T, Wang L Q, et al. Tempo-spatial variations of Mesozoic magmatic rocks in the Gangdese belt, Tibet, China, with a discussion of geodynamic setting-related issues (in Chinese with English abstract). Geol Bull China, 2008, 27(9): 1535－1550

18 Guynn J H, Kapp P, Pullen A, et al. Tibetan basement rocks near Amdo reveal "missing" Mesozoic tectonism along the Bangong suture, central Tibet. Geology, 2006, 34: 505－508

19 Kapp P, Murphy M A, Yin A. Mesozoic and Cenozoic tectonic evolution of the Shiquanhe area of western Tibet. Tectonics, 2003, 22: 1029, doi: 10.1029/2001TC001332

20 Volkmer J E, Kapp P, Guynn J H, et al. Cretaceous-Tertiary structural evolution of the north central Lhasa Terrane, Tibet. Tectonics, 2007, 26: TC6007, doi: 6010.1029/2005TC001832

21 Hu D G, Wu Z H, Jiang W, et al. SHRIMP zircon U-Pb age and Nd isotopic study on the Nyainqêntanglha Group in Tibet. Sci China Ser D-Earth Sci, 2005, 48(9): 1377－1386

22 He S D, Kapp P, DeCelles P G, et al. Cretaceous-Tertiary geology of the Gangdese Arc in the Linzhou area, southern Tibet. Tectonophysics, 2007, 433: 15－37

23 Coulon C, Maluski H, Bollinger C, et al. Mesozoic and Cenozoic volcanic rocks from central and southern Tibet: $^{39}Ar/^{40}Ar$ dating, petrological characteristics and geodynamical significance. Earth Planet Sci Lett, 1986, 79: 281－302

24 Chung S L, Chu M F, Zhang Y Q, et al. Tibetan tectonic evolution inferred from spatial and temporal variations in post-collisional magmatism. Earth Sci Rev, 2005, 68: 173－196

25 Kapp P, Yin A, Harrison T M. Cretaceous-Tertiary shortening, basin development, and volcanism in central Tibet. Geol Soc Am Bull, 2005, 117: 865－878

26 Chu M F, Chung S L, Song B. Zircon U-Pb and Hf isotope constraints on the Mesozoic tectonics and crustal evolution of southern Tibet. Geology, 2006, 34: 745－748

27 Bureau of Geology and Mineral Resources of Xizang Autonomous Region. Regional Geology of Xizang (Tibet) Autonomous Region (in Chinese with English abstract). Beijing: Geological Publishing House, 1993. 378－379

28 Copeland P, Harrison T M, Pan Y. et al. Thermal evolution of the Gangdese batholith, southern Tibet: A history of episodic unroofing. Tectonics, 1995, 14: 223－236

29 Wen D R, Liu D Y, Chung S L, et al. Zircon SHRIMP U-Pb ages of the Gangdese Batholith and implications for Neotethyan subduction in southern Tibet. Chem Geol, 2008, 252: 191－201

30 Zhu D C, Pan G T, Zhao Z D, et al. Early Cretaceous subduction-related adakite-like rocks in the Gangdese, south Tibet: Products of slab melting and subsequent melt-peridotite interaction? J Asian Earth Sci, 2009, 34: 298－309

31 Ji W Q, Wu F Y, Chung S L. Zircon U-Pb chronology and Hf isotopic constraints on the petrogenesis of Gangdese batholiths, southern Tibet. Chem Geol, 2009, 262: 229－245

32 Liang Y H, Chung S L, Liu D Y, et al. Detrital zircon evidence from Burma for reorganization of the eastern Himalayan river system. Am J Sci, 2008, 308: 618－638

33 Chiu H Y, Chung S L, Wu F Y, et al. Zircon U-Pb and Hf isotope constraints from eastern Transhimalayan batholiths on the precollisional magmatic and tectonic evolution in southern Tibet. Tectonophysics, 2009, doi: 10.1016/j.tecto.2009.02.034

34 Peng X J, Chen Y M, Zhang S Q. Paleoproterozoic Demala Group in the Zayu area, Tibet (in Chinese with English abstract). Region Geol China, 1999, 18(2): 148－154

35 Liu M, Zhu D C, Zhao Z D, et al. Early Cretaceous magma mixing in Ranwu area of eastern Gangdese, Tibet: Evidence from zircon SHRIMP U-Pb age and Hf isotopic composition (in Chinese with English abstract). Earth Sci Front, 2009, 16(2): 152－160

36 Lin I J. Geochemical Constraints on the Petrogenesis of Cretaceous to Paleocene Granitoids and Volcanic Rocks from SE Tibet (in Chinese with English abstract). Master Thesis. Taipei: Taiwan University, 2007. 1－81

37 Liu D Y, Jian P, Kröner A, et al. Dating of prograde metamorphic events deciphered from episodic zircon growth in rocks of the

Dabie-Sulu UHP complex, China. Earth Planet Sci Lett, 2006, 250: 650－666
38 Gao S, Liu X M, Yuan H L, et al. Determination of forty-two major and trace elements of USGS and NIST SRM glasses by LA-ICPMS. Geostand Newsl, 2002, 26: 181－195
39 Zhang H F, Gao S, Zhong Z Q, et al. Geochemical and Sr-Nd-Pb isotopic compositions of Cretaceous granitoids: Constraints on tectonic framework and crustal structure of the Dabieshan ultrahigh pressure metamorphic belt, China. Chem Geol, 2002, 186: 281－299
40 Keto L S, Jacobsen S B. Nd and Sr isotopic variations of Early Paleozoic oceans. Earth Planet Sci Lett, 1987, 84: 27－41
41 Watson E B, Harrison T M. Zircon saturation revisited: Temperature and composition effects in a variety of crustal magma types. Earth Planet Sci Lett, 1983, 64: 295－304
42 Wu F Y, Yang Y H, Xie L W, et al. Hf isotopic compositions of the standard zircons and baddeleyites used in U-Pb geochronology. Chem Geol, 2006, 234: 105－126
43 Xie L W, Zhang Y B, Zhang H H, et al. In situ simultaneous determination of trace elements, U-Pb and Lu-Hf isotopes in zircon and baddeleyite. Chin Sci Bull, 2008, 53(10): 1565－1573
44 Soderlund U, Patchett P J, Vervoort J D, et al. The ^{176}Lu decay constant determined by Lu-Hf and U-Pb isotope systematics of Precambrian mafic intrusions. Earth Planet Sci Lett, 2004, 219: 311－324
45 Griffin W L, Wang X, Jackson S E, et al. Zircon chemistry and magma mixing, SE China: In-situ analysis of Hf isotopes, Tonglu and Pingtan igneous complexes. Lithos, 2002, 61: 237－269
46 Blichert-Toft, J, Albarède, F. The Lu-Hf geochemistry of chondrites and the evolution of the mantle-crust system. Earth Planet Sci Lett, 1997, 148: 243－258
47 Griffin W L, Pearson N J, Belousova E. et al, The Hf isotope composition of cratonic mantle: LAM-MC-ICPMS analysis of zircon megacrysts in kimberlites. Geochim Cosmochim Acta, 2000, 64: 133－147
48 Li X H, Li Z X, Li W X, et al. U-Pb zircon, geochemical and Sr-Nd-Hf isotopic constraints on age and origin of Jurassic I- and A-type granites from central Guangdong, SE China: A major igneous event in response to foundering of a subducted flat-slab? Lithos, 2007, 96: 186－204
49 Streckeisen A, Le Maitre R W. A chemical approximation to the modal QAPF classification of the igneous rocks. N Jb Miner Abh, 1979, 136: 169－206
50 Whalen J B, Currie K L, Chappell B W. A-type granites: Geochemical characteristics, discrimination and petrogenesis. Contrib Mineral Petrol, 1987, 95: 407－419
51 Sun S S, McDonough W F. Chemical and isotope systematics of oceanic basalts: implications for mantle composition and processes. In: Saunders A D, eds. Magmatism in Ocean Basins. Geol Soc Publ, 1989, 42: 313－345
52 Liu Q S, Jiang W, Jian P, et al. Zircon SHRIMP U-Pb age and petrochemical and geochemical features of Mesozoic muscovite monzonitic granite at Ningzhong, Tibet (in Chinese with English abstract). Acta Petrol Sin, 2006, 22(3): 643－652
53 Rudnick R L, Gao S. The Composition of the Continental Crust. In: Holland H D, Turekian K K, eds. Treatise on Geochemistry. Oxford: Elsevier-Pergamon, 2003. 1－64
54 Wu F Y, Li X H, Zheng Y F, et al. Lu-Hf isotopic systematics and their applications in petrology (in Chinese with English abstract). Acta Petrol Sin, 2007, 23(2): 185－220
55 Schwab M, Ratschbacher L, Siebel W, et al. Assembly of the Pamirs: age and origin of magmatic belts from southern Tien Shan to the southern Pamirs and their relation to Tibet. Tectonics, 2004, 23: TC4002
56 Lee H Y, Chung S L, Lo C H, et al. Eocene Neotethyan slab breakoff in southern Tibet inferred from the Linzizong volcanic record. Tectonophysics, 2009, doi: 10.1016/j.tecto.2009.02.031
57 He Z H, Yang D M, Wang T W. The determination of early Cretaceous post-collision granitoids in Sangba area of Gangdese tectonic belt and its tectonic significance (in Chinese with English abstract). Acta Petrol Mineral, 2006, 25(3): 185－193
58 Wolf M B, London D. Apatite dissolution into peraluminous haplogranitic melts: An experimental study of solubilities and mechanism. Geochim Cosmochim Acta, 1994, 58: 4127－4145
59 Chappell B W. Aluminium saturation in I- and S-type granites and the characterization of fractionated haplogranites. Lithos, 1999, 46: 535－551
60 Wu F Y, Jahn B M, Wilder S A, et al. Highly fractionated I-type granites in NE China (I): Geochronology and petrogenesis. Lithos, 2003, 66: 241－273
61 Li X H, Li Z X, Li W X, et al. Initiation of the Indosinian Orogeny in South China: Evidence for a Permian magmatic arc in the Hainan Island. J Geol, 2006, 114: 341－353
62 Li X H, Li W X, Li Z H. On the genetic classification and tectonic implications of the Early Yanshanian granitoids in the Nanling Range, South China. Chin Sci Bull, 2007, 52 (14): 1873－1885
63 Kemp A I S, Hawkesworth C J, Foster G L. et al. Magmatic and crustal differentiation history of granitic rocks from Hf-O isotopes in zircon. Science, 2007, 315: 980－983
64 Bolhar R, Weaver S D, Whitehouse M J, et al. Sources and evolution of arc magmas inferred from coupled O and Hf isotope systematics of plutonic zircons from the Cretaceous Separation Point Suite (New Zealand). Earth Planet Sci, 2008, 268: 312－324
65 Beloisova B A, Griffin W L, O'Reilly S Y. Zircon crystal morphology, trace element signatures and Hf isotope composition as a tool for petrogenetic modeling: Examples from Eastern Australian granitoids. J Petrol, 2006, 47: 329－353
66 Yang J H, Wu F Y, Wilde, S A, et al. Tracing magma mixing in granite genesis: *In situ* U-Pb dating and Hf-isotope analysis of zircons. Contrib Mineral Petrol, 2007, 153: 177－190
67 Chappell B W, Stephens W E. Origin of infracrustal (I-type) granite magmas. Trans R Soc Edinburgh: Earth Sci, 1988, 79(2-3): 71－86
68 Collins W J, Richards S W. Geodynamic significance of S-type granites in circum-Pacific orogens. Geology, 2008, 36: 559－562
69 Zhang H F, Harris N, Parrish R, et al. Causes and consequences of protracted melting of the mid-crust exposed in the North Himalayan antiform. Earth Planet Sci Lett, 2004, 228: 195－212
70 Kapp P, DeCelles P G, Gehrels G E, et al. Geological records of the Lhasa-Qiangtang and Indo-Asian collisions in the Nyima area of central Tibet. Geol Soc Am Bull, 2007, 119: 917－932
71 Leier A L, Kapp P, Gehrels G E, et al. Detrital zircon geochronology of Carboniferous-Cretaceous strata in the Lhasa Terrane, Southern Tibet. Basin Res, 2007, 19: 361－378